Different types of chimera states: An interplay between spatial and dynamical chaos

Dawid Dudkowski,[1] Yuri Maistrenko,[1,2] and Tomasz Kapitaniak[1]

[1]*Division of Dynamics, Technical University of Lodz, Stefanowskiego 1/15, 90-924 Lodz, Poland*

[2]*Institute of Mathematics and Centre for Medical and Biotechnical Research, National Academy of Sciences of Ukraine,*
Tereshchenkivska Street 3, 01030, Kyiv, Ukraine

(Received 7 July 2014; published 23 September 2014)

We discuss the occurrence of chimera states in networks of nonlocally coupled bistable oscillators, in which individual subsystems are characterized by the coexistence of regular (a fixed point or a limit cycle) and chaotic attractors. By analyzing the dependence of the network dynamics on the range and strength of coupling, we identify parameter regions for various chimera states, which are characterized by different types of chaotic behavior at the incoherent interval. Besides previously observed chimeras with space-temporal and spatial chaos in the incoherent intervals we observe another type of chimera state in which the incoherent interval is characterized by a central interval with standard space-temporal chaos and two narrow side intervals with spatial chaos. Our findings for the maps as well as for time-continuous van der Pol–Duffing's oscillators reveal that this type of chimera states represents characteristic spatiotemporal patterns at the transition from coherence to incoherence.

The coexistence of coherent and incoherent structures in networks of coupled oscillators, known as the chimera states, is a widely occuring phenomenon in nature. First observed by Kuramoto [1], it was later studied by many scientists and today is one of the fastest growing branches of dynamical systems and networks theory. The works on chimeras relate to a variety of models like phase oscillators [2–7] (for which they were originally found), chemical oscillators [8,9], neuron models [10], planar oscillators [11], and many other different types of networks [12–24]. Chimera states are well known for nonlocally coupled systems, but recently they also have been found in feedback-delayed oscillators [25–27] and in globally coupled networks [18,19]. The coherence-incoherence transitions [28,29], spatiotemporal patterns [31], chaotic transients [32], and spectral properties [33] are only a few of recent studies on chimera states. Interesting studies about different chimera variants can be found in Refs. [27,34–37] (e.g., multiclustered chimera states and their cascades [23,34], virtual chimera states [27], controlling chimeras [21,22], and two-dimensional chimera states [5,16,17,24,36]). In Ref. [38] a real physical experiment on chimeras in mechanical oscillator networks is presented.

Depending on the dynamics of the oscillators at incoherent intervals two types of chimera states have been identified. In the incoherent intervals of the first type (chimera type I) one observes space-temporal chaos characterized by hyperchaotic behavior with many positive Lyapunov exponents [33]. This type of chimera state is widely observed for networks of continuous time nodes (given by differential equations, e.g., complex Ginzburg-Landau equations or Kuramoto model [1–8]). In the second type (chimera type II) only spatial chaos is observed in the chimera's incoherent interval such that the temporal dynamics is very simple, in most cases periodic. This type has been observed in networks of discrete time nodes (maps) [28–30] but recently also for time-continuos Stuart-Landau oscillators [37].

Our paper gives the link between these two types of chimera states. We identify another chimera state (chimera type III) in which the incoherent interval is characterized

by a central interval with standard space-temporal chaos and two narrow side intervals with spatial chaos. Therefore, we have obtained a hybrid chimera state, where the behavior at the incoherent interval splits up into two intervals with very different behaviors, namely space-temporal chaos and spatial chaos. In some sense, this could be considered as the second hierarchical level of the chimera state (the chimera's incoherent interval is divided into two smaller ones with incongruent behavior inside).

In this paper we study the interplay between coherent and incoherent dynamics in networks of nonlocally coupled oscillators. Contrary to most previous studies, where networks with monostable (one attractor) units have been considered, we focus on networks of the oscillators with coexisting attractors. We consider bistable units with coexisting chaotic and regular attractors. Such an approach can extend our knowledge about the chimera states phenomenon.

We start with coupled bistable maps

$$x_{t+1}^i = f(x_t^i) + \frac{d}{2P} \sum_{j=i-P}^{i+P} \left[f(x_t^j) - f(x_t^i) \right], \qquad (1)$$

where x^i are real dynamic variables ($i = 1, \ldots, N$ and index i is periodic mode N), t denotes discrete time, d is the coupling parameter, $2P$ is the number of neighbors in both directions coupled with the ith map, and function f describes a one-dimensional system. We choose f as the piecewise linear map

$$f(x) = \begin{cases} p_1 x + (p_1/l - 1) & : x \in [-1, -1/l) \\ lx & : x \in [-1/l, 1/l) \\ p_2 x - (p_2/l - 1) & : x \in [1/l, 1] \end{cases} \qquad (2)$$

where p_1, l, p_2 are the slopes of linear functions described in intervals $[-1, -1/l), [-1/l, 1/l)$, and $[1/l, 1]$ respectively. f is a bistable map for certain parameters, namely $-1 < p_1 < 0, l > 1, p_2 < -1$, when the stable fixed point coexists with the chaotic attractor. Previously, this kind of coupled maps has been studied in Ref. [39], where the symmetrical case ($p_1 = p_2$) when both coexisting attractors are chaotic has been considered. In our studies we fixed p_1 and p_2, essentially
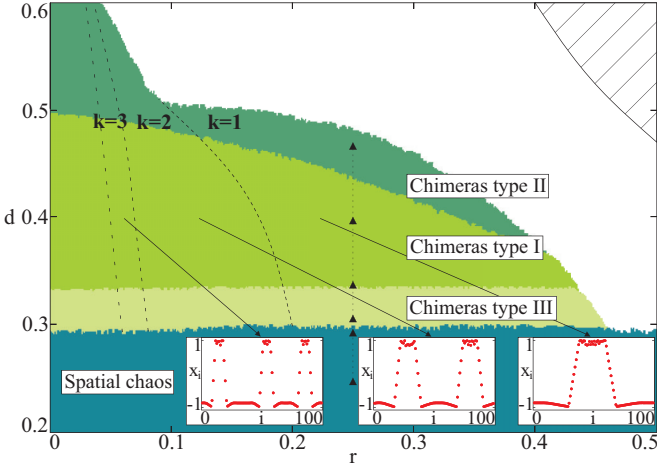
FIG. 1. (Color online) Regions of various behaviors for system (1) in the (r,d) parameter space. Each color (grayscale) and signature refers to a different state of the system, with complete synchronization marked as the hatched region. The $k = 1,2,3,\ldots$ numbers denote the regions of different chimera's heads, which are separated by the dotted lines. The snapshots of typical chimera states of the second type are shown in the insets. Parameters: $l = 1.5, p_1 = -0.5, p_2 = -2.4$, $N = 100$.

different choosing the parameters as $p_1 = -0.5, p_2 = -2.4$, and $l = 1.5$, and for such parameters there exist (i) equilibrium $x_0 = -8/9$ with its basin of attraction as interval $[-1,0)$ and (ii) chaotic attractor $A = [0.2,1]$ with its basin of attraction as interval $(0,1]$.

The results of direct numerical simulations of Eqs. (1) and (2) in the two-parameter plane of the coupling radius $r = P/N$ and coupling strength d are presented in Fig. 1. When r and d are sufficiently large, all maps synchronize on one of two coexisting attractors. It can be a stable fixed point x_0 (there is no dynamics) or chaotic attractor A when complete chaotic synchronization of the system occurs. The region of complete synchronization is marked as hatched. On the other hand, if the coupling parameter is small enough, then for any coupling radius we obtain spatial chaos [28,40,41]. Even though individual oscillators are coupled in the network with appropriate choice of initial conditions they get attracted directly to those of two attractors which basins they initially start from. Therefore, the number of coexisting network attractors is exponentially large, growing with the system's size N (in this case equal to 2^N). Any coherent, self-organized structures do not exist in the system (except of these given by stable fixed point x_0). The chimera states are observed for intermediate values of the coupling coefficient d and these regions are denoted by "Chimeras type I–III." The colors (shades of gray) denote different chimera types.

The typical bifurcation scenario of the transition between different chimera states is presented in Fig. 2, where we fix the coupling radius $r = 0.25$ and increase the coupling strength d along the vertical line with triangles in Fig. 1. Figures 2(a)–2(f) refer to the points marked as black triangles in Fig. 1 [with panel (a) $d = 0.25$ referring to the lower triangle and panel (f) $d = 0.47$ to the top one]. In the left column the snapshots after transient time $t = 20000$ are shown, while in the right
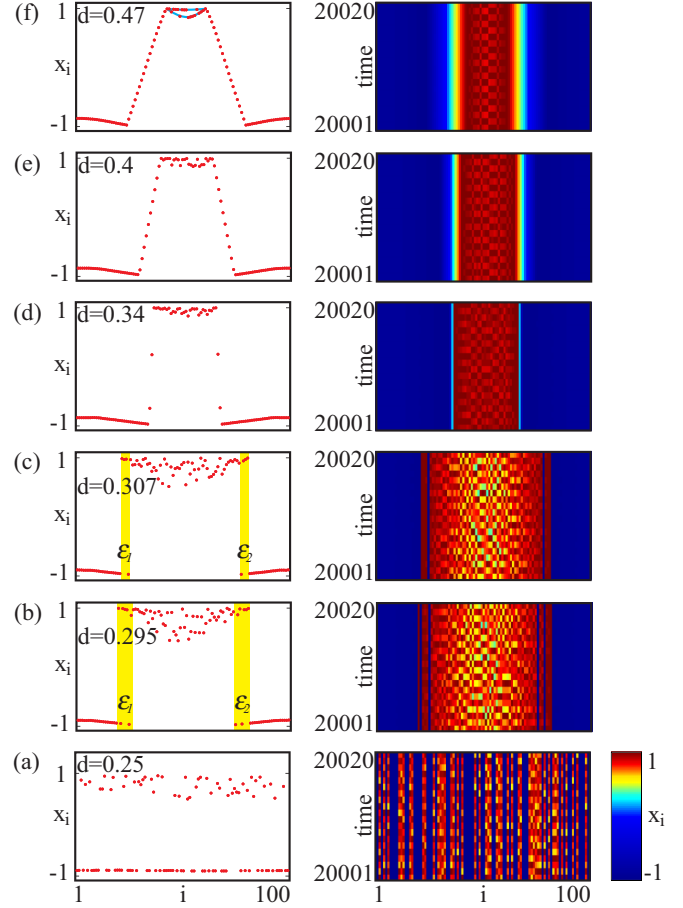

FIG. 2. (Color online) Typical bifurcation scenario for network (1,2) with fixed coupling radius $r = 0.25$ (black triangles in Fig. 1). For each value of the coupling strength d (increasing from the bottom to the top, $d = 0.25, 0.295, 0.307, 0.34, 0.4, 0.47$ respectively) the snapshots (left column) and space-time plots (right column) are shown. Other parameters as in Fig. 1.

column space-time plots of the next 20 iterations are presented. Each panel in Fig. 2 has been made for different coupling parameters, starting with randomly chosen initial conditions.

Figure 1 has been calculated in the following way: We start at point (r,d) inside the region of spatial chaos and increase d. Each point inside this region has been iterated for 100 randomly chosen initial conditions. Point (r,d) with the smallest d for which we find at least one chimera state has been assumed as the boundary point between spatial chaos and chimera type III regions. Over this boundary the calculations have been performed using the continuation method (calculations for each new value of d have started with the chimera state observed for previous d value). The lower boundaries of the chimera type I and II regions have been determined by the lowest values of d for which respectively chimera type III transform into chimera type I or chimera type I into chimera type II. The d values for which none of chimera types survive determine the upper blank region.

First, when the value of coupling equals $d = 0.25$, spatial chaos is observed [Fig. 2(a)]: The oscillators are placed close to the attractors from which they have started. This network state

radically changes for $d = 0.295$ [Fig. 2(b)] when chimera type III appear. Three essentially different (incongruent) structures are created in the network: one coherent and two incoherent ones. The coherent one is the lower cluster, where the maps stay close to fixed point x_0. The incoherent structure is in the upper middle part of the snaphot, where the oscillators are desynchronized and temporal chaos occurs. There is also the second incoherent structure in between these two, marked as shaded yellow (light gray) stripes ε_1 and ε_2. In the state, we observe spatial chaos combined with temporal one. Indeed, the oscillators are distributed between lower and upper parts in a random way (the distribution is given by the initial conditions) such that these above behave chaotically in time whereas those which are below are "almost not moving." It has to be emphasized that not every combination of maps (network units) in the incoherent part can be realized by the appropriate choice of initial conditions. Usually, if we exchange the initial condition in the region for a single oscillator only (with other initial conditions unchanged), the whole structure is destroyed and the system transforms into a different chimera state.

With further increase of coupling strength d, the spatial chaos stripes become narrower [Fig. 2(c)] and at some bifurcation value, they shrink and disappear. Chimera type I like the ones shown in Fig. 2(d) are born. Both the lower cluster and the upper incoherent part with dynamical chaos have survived but the amplitude of the chaotic oscillations of the upper part becomes smaller. In addition, both structures coherent and incoherent are connected with a smooth (almost linear) profile, as one may observe in Figs. 2(d) and 2(e) at the place of the disappearing yellow (light gray) stripes. The transitional zone between coherence and incoherence becomes wider with further increase of d, as illustrated in Figs. 2(d) and 2(e). Finally, when the boundary of this parameter region is reached, chimeras type II appear with spatial chaos at the incoherence region. Indeed, as one can see in Fig. 2(f), the maps (network units) are "randomly" located in space at two branches (upper and lower curves on the snapshot) and with next iterations each unit jumps from one branch to another and backwards. For various initial conditions exponentially many (with N) combinations of these locations can be obtained, including a peculiar case when all the maps are placed at one of the branches only (and then all together periodically jump between two branches).

With further increase of the coupling coefficient d, we leave the region of chimera states and the whole network dynamics ends at one of the two attractors of the piecewise linear map, Eq. (2). This parameter area is left blank in Fig. 1. When the attractor for all the maps is chaotic, it is known that chimeras type II can arise for nonlocally coupled unimodal maps in appropriate parameter regions [28,29].

Regions for chimera states in Fig. 1 are divided by the dotted lines which determine the additional subregions signed by $k = 1,2,3$ numbers. These numbers refer to the number of the so-called chimeras heads (i.e., the regions of chaoticity) [4]; characteristic examples are illustrated in the insets. Further decrease of r yields additional higher order regions of multiheaded chimera states following the head-adding cascade $k = 4,5,\dots$ (not shown in Fig. 1).

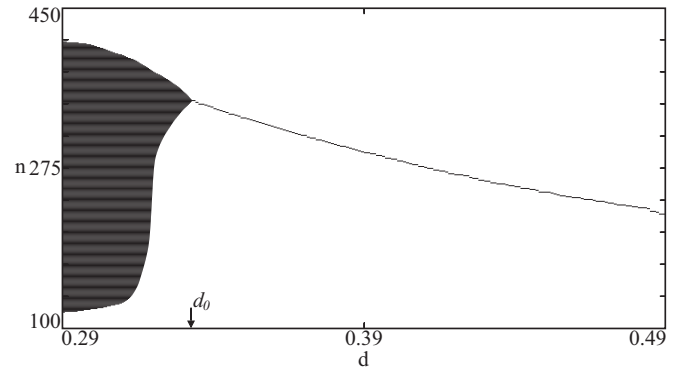To investigate the multiplicity of the chimera states, we analyzed all possible structures obtained from many random

FIG. 3. Multiplicity and uniqueness of chimera states for network (1,2) with fixed coupling radius $r = 0.25$. Parameter n denotes a number of maps attracted to the lower branch of chimera, which can change widely for $d < d_0$. For $d \geqslant d_0$ states are unique. $N = 500$ units have been considered. Other parameters as in Fig. 1.

initial conditions at the transition when chimeras type III are born. The results are presented in Fig. 3. Here n denotes the number of units attracted to the lower cluster (units in equilibria). As shown in Fig. 3 n can take various values as $d \in [0.29, d_0]$ and then many different chimera type III exist. With the coupling increase the multiplicity declines and eventually for $d > d_0$ a unique chimeras type I is observed (for all larger coupling values where it exists). To our surprise, the multiplicity bifurcation point d_0 seems to be independent of the coupling radius r and in our numerical simulations equals $d_0 \cong 0.334$.

To test if the bifurcation transitions between different types of the chimera states are a universal scenario, we have also investigated nonlocally coupled networks of bistable units with different local dynamics. Figure 4 illustrates the bifurcation transition for nonlocally coupled piecewise logistic function f:

$$f(x) = \begin{cases} a_1 x(1 + x) & : x \in [-1, 0) \\ a_2 x(1 - x) & : x \in [0, 1] \end{cases}. \quad (3)$$

The bifurcation parameters a_1, a_2 are fixed at the values $a_1 = 2.5$ (equilibrium) and $a_2 = 3.8$ (chaotic attractor). Then for $x \in (0, 1]$ we have a chaotic logistic map and the chimera state appearance in this case has been derived in Refs. [28,29]. For $x \in [-1, 0]$ the dynamics of f is trivial given by a stable fixed point.

As the second example we consider the nonlocally coupled van der Pol–Duffing oscillators with external excitation:

$$\dot{x}_i = y_i + \frac{d}{2P} \sum_{j=i-P}^{i+P} [x_j - x_i]$$

$$\dot{y}_i = \alpha (1 - x_i^2) y_i - x_i^3 + F \sin \omega t$$

$$+ \frac{d}{2P} \sum_{j=i-P}^{i+P} [y_j - y_i] \quad (4)$$

where α, F, and ω are constant. As shown in Ref. [42], individual dynamics of the oscillators in system (4) is very rich; for various parameter values it can be mono-, bi- or multistable
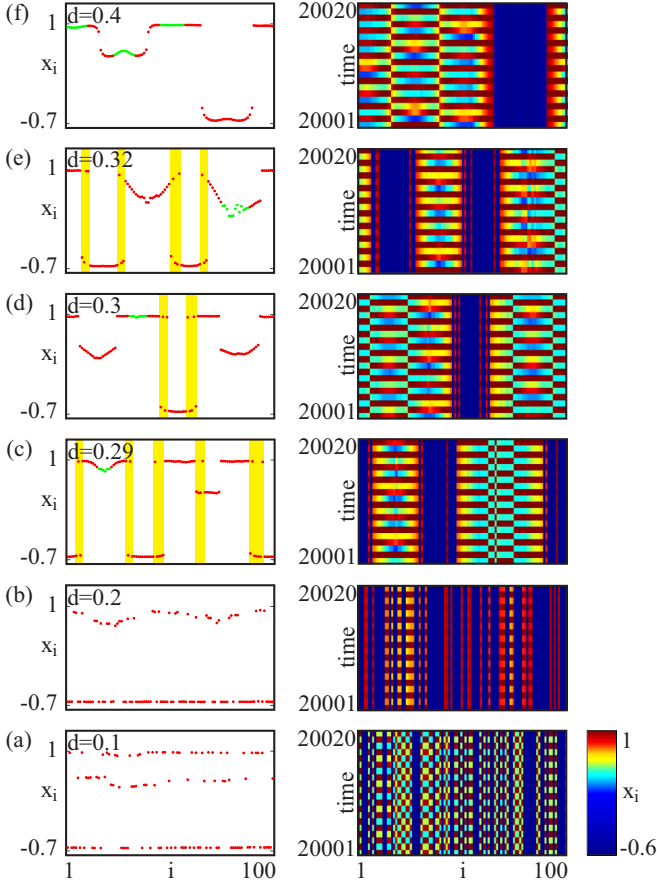
FIG. 4. (Color online) Snapshots (left column) and space-time plots (right column) for Eqs. (1) and (3) of coupled piecewise logistic maps. Coupling strength increases from the bottom to the top, $d = 0.1, 0.2, 0.29, 0.3, 0.32, 0.4$ respectively. Parameters: $a_1 = 2.5, a_2 = 3.8, N = 100, r = 0.1$. Observed states correspond to dynamics of Eqs. (1) and (2). In upper structures in chimera states [Figs. 4(c)–4(e)] units can oscillate periodically with different periods (red [dark gray] dots on the snapshots) or chaotically (green [light gray] dots on the snapshots).
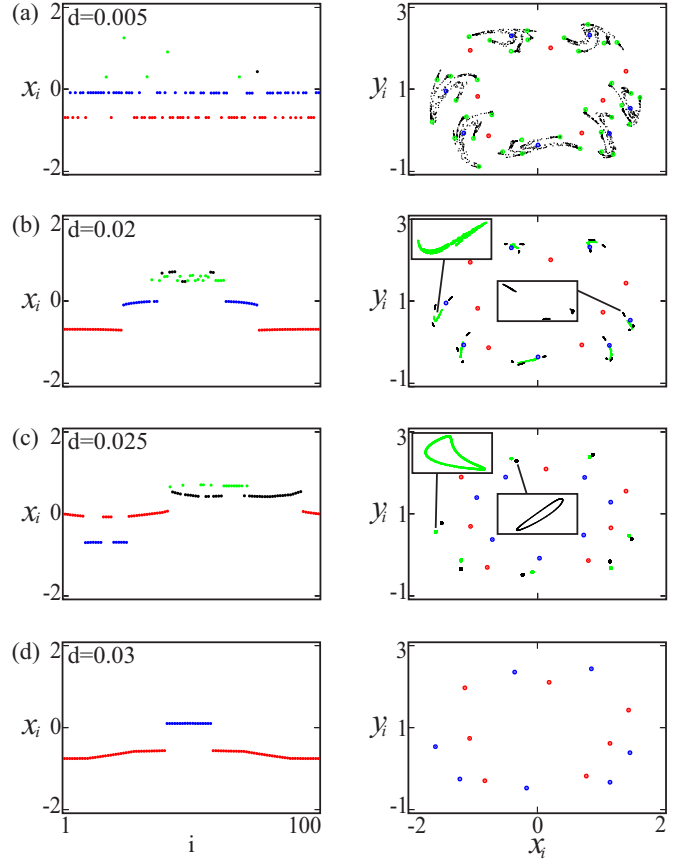

FIG. 5. (Color online) Snapshots (left column) and Poincaré maps (right column) of the oscillators of network (5). For each subfigure (a)–(d) colors denoting oscillators on the snapshot refer to the attractors shown on the map where the corresponding oscillators are located. For periodic solutions (finite number of dots) period is equal to number of dots on map multiplied by $2\pi/0.94$ (period of the external excitation). Parts of quasiperiodic and chaotic attractors in panels (b) and (c) are enlarged in the insets. Parameters: $N = 100$, $r = 0.1$.

with different types of regular and chaotic attractors. In our simulations we fix parameters $\alpha = 0.2, F = 1$, and $\omega = 0.94$, for which the oscillators are bistable, having one periodic and one chaotic attractor. It should be noted that there are two coupling components in Eq. (4), one for the position coordinates [the first equation in Eq. (4)] and the second for the velocity [the second equation in Eq. (4)].

The dynamics of system (5) is shown in Fig. 5. For the small coupling there are three periodic and one chaotic attractors [Fig. 5(a), right panel], and the network dynamics is developed in the form of spatial chaos only [Fig. 5(a), left panel] such that chimera states occur for larger d values. As one can observe in Fig. 5(b), two levels of clusters are created (with periodic dynamics) but there are also incoherent parts with chaotic oscillations (an enlargement is shown in the inset). When the coupling coefficient increases further [Fig. 5(c)], the branches of periodic solutions remain, but chaotic dynamics transforms into a quasiperiodic one. With further increase of d the irregular behavior disappears and chimeras are not observed any more [Fig. 5(d)].

In conclusion, we have identified a different type of chimera states in networks with nonlocally coupled bistable systems. This type of behavior is observed in a wide range of coupling parameters and is characterized by the central interval with standard space-temporal chaos and two narrow side intervals with spatial chaos inside chimera's incoherent interval. We have found similar patterns for coupled maps (piecewise linear and logistic) as well as for time-continuous systems. This indicates a common, possibly universal phenomenon in networks of very different nature due to the bistability of individual oscillators. The studies of the dynamics of networks of multistable units, in which new types of chimeras' states appear, can lead to better understanding of the transition between coherence and incoherence in the systems of very different nature.

[1] Y. Kuramoto and D. Battogtokh, Nonlinear Phenom. Complex Syst. **5**, 380 (2002).

[2] D. M. Abrams and S. H. Strogatz, Phys. Rev. Lett. **93**, 174102 (2004).

[3] D. M. Abrams and S. H. Strogatz, Int. J. Bifur. Chaos Appl. Sci. Engrg. **16**, 21 (2006).

[4] Y. L. Maistrenko, A. Vasylenko, O. Sudakov, R. Levchenko, and V. L. Maistrenko, Int. J. Bifurcation Chaos Appl. Sci. Engry. **24**, 1440014 (2014).

[5] O. E. Omel'chenko, M. Wolfrum, S. Yanchuk, Y. L. Maistrenko, and O. Sudakov, Phys. Rev. E **85**, 036210 (2012).

[6] G. C. Sethia, A. Sen, and F. M. Atay, Phys. Rev. Lett. **100**, 144102 (2008).

[7] C. R. Laing, Phys. D (Amsterdam, Neth.) **238**, 1569 (2009).

[8] M. R. Tinsley, S. Nkomo, and K. Showalter, Nat. Phys. **8**, 662 (2012).

[9] S. Nkomo, M. R. Tinsley, and K. Showalter, Phys. Rev. Lett. **110**, 244102 (2013).

[10] J. Hizanidis, V. G. Kanas, A. Bezerianos, and T. Bountis, Int. J. Bifur. Chaos Appl. Sci. Engrg. **24**, 1450030 (2014).

[11] C. R. Laing, Phys. Rev. E **81**, 066221 (2010).

[12] H. Wang and X. Li, Phys. Rev. E **83**, 066214 (2011).

[13] T. Bountis, V. G. Kanas, J. Hizanidis, and A. Bezerianos, Eur. Phys. J. Spec. Top. **223**, 721 (2014).

[14] C. R. Laing, Chaos **19**, 013113 (2009).

[15] D. M. Abrams, R. Mirollo, S. H. Strogatz, and D. A. Wiley, Phys. Rev. Lett. **101**, 084103 (2008).

[16] M. J. Panaggio and D. M. Abrams, arXiv:1405.2047.

[17] E. A. Martens, C. R. Laing, and S. H. Strogatz, Phys. Rev. Lett. **104**, 044101 (2010).

[18] L. Schmidt, K. Schönleber, K. Krischer, and V. Garcia-Morales, Chaos **24**, 013102 (2014).

[19] A. Yeldesbay, A. Pikovsky, and M. Rosenblum, Phys. Rev. Lett. **112**, 144103 (2014).

[20] G. C. Sethia and A. Sen, Phys. Rev. Lett. **112**, 144101 (2014).

[21] J. Sieber, O. E. Omel'chenko, and M. Wolfrum, Phys. Rev. Lett. **112**, 054102 (2014).

[22] C. Bick and E. A. Martens, arXiv:1402.6363.

[23] J. Xie, E. Knobloch and H.-C. Kao, Phys. Rev. E **90**, 022919 (2014).

[24] M. J. Panaggio and D. M. Abrams, arXiv:1403.6204.

[25] O. E. Omel'chenko, Y. L. Maistrenko, and P. A. Tass, Phys. Rev. Lett. **100**, 044105 (2008).

[26] J. H. Sheeba, V. K. Chandrasekar, and M. Lakshmanan, Phys. Rev. E **79**, 055203 (2009).

[27] L. Larger, B. Penkovsky, and Y. Maistrenko, Phys. Rev. Lett. **111**, 054103 (2013).

[28] I. Omelchenko, Y. Maistrenko, P. Hövel, and E. Schöll, Phys. Rev. Lett. **106**, 234102 (2011).

[29] I. Omelchenko, B. Riemenschneider, P. Hövel, Y. Maistrenko, and E. Schöll, Phys. Rev. E **85**, 026212 (2012).

[30] A. M. Hagerstrom, T. E. Murphy, R. Roy, P. Hövel, I. Omelchenko, and E. Schöll, Nat. Phys. **8**, 658 (2012).

[31] O. E. Omel'chenko, M. Wolfrum, and Y. L. Maistrenko, Phys. Rev. E **81**, 065201(R) (2010).

[32] M. Wolfrum and O. E. Omel'chenko, Phys. Rev. E **84**, 015201(R) (2011).

[33] M. Wolfrum, O. E. Omel'chenko, S. Yanchuk, and Y. L. Maistrenko, Chaos **21**, 013112 (2011).

[34] I. Omelchenko, O. E. Omel'chenko, P. Hövel, and E. Schöll, Phys. Rev. Lett. **110**, 224101 (2013).

[35] Y. Kawamura, Phys. Rev. E **75**, 056204 (2007).

[36] M. J. Panaggio and D. M. Abrams, Phys. Rev. Lett. **110**, 094102 (2013).

[37] A. Zakharova, M. Kapeller, and E. Schöll, Phys. Rev. Lett. **112**, 154101 (2014).

[38] E. A. Martens, S. Thutupalli, A. Fourriere, and O. Hallatschek, Proc. Natl. Acad. Sci. USA **110**, 10563 (2013).

[39] Y. Maistrenko and T. Kapitaniak, Phys. Rev. E **54**, 3285 (1996).

[40] L. P. Nizhnik, I. L. Nizhnik, and M. Hasler, Int. J. Bifur. Chaos Appl. Sci. Engrg. **12**, 261 (2002).

[41] W. Shen, SIAM J. Appl. Math. **56**, 1379 (1996).

[42] A. Chudzik, P. Perlikowski, A. Stefanski, and T. Kapitaniak, Int. J. Bifur. Chaos Appl. Sci. Engrg. **21**, 1907 (2011).